

Asymptotic Data Rates of Receive-Diversity Systems with MMSE Estimation and Spatially Correlated Interferers

Siddharta Govindasamy, Member

Abstract

An asymptotic technique is presented to characterize the bits/symbol achievable on a representative wireless link in a spatially distributed network with active interferers at correlated positions, N receive diversity branches, and linear Minimum-Mean-Square-Error (MMSE) receivers. This framework is then applied to systems including analogs to Matern type I and type II networks which are useful to model systems with Medium-Access Control (MAC), cellular uplinks with orthogonal transmissions and frequency reuse, and Boolean cluster networks. It is found that for our network models, with moderately large N , the correlation between interferer positions does not significantly influence the bits/symbol resulting in simple approximations for the data rates achievable in such networks which are known to be difficult to analyze and for which few analytical results are available.

Index Terms

Matern, MIMO, MMSE, Cellular, Reuse.

I. INTRODUCTION

In systems with multiple diversity branches such as multi-antenna systems, the diversity can be used for interference mitigation which can improve spatial reuse, and increase aggregate data rates in networks. Since signal and interference strengths are influenced by relative node positions, the spatial distribution of nodes strongly influences the performance of such systems. Most works on wireless networks with spatially distributed nodes assume that the locations of active nodes are independent, a good model for networks with uncoordinated transmissions (e.g. [1], [2], [3], [4], [5]). In many situations however, active nodes may be spatially correlated, e.g. in networks with coordinated transmissions such as networks with Medium-Access-Control (MAC), systems with significant physical constraints on how close nodes may get to each other such as vehicular networks, networks which employ location-based spatial reuse such as cellular networks, and networks with spatially clustered users. The analysis of networks with spatially correlated transmitters is well known to be difficult¹.

In this paper, we develop an asymptotic technique to characterize the Signal-to-Interference-Ratio (SIR) of a representative link with multiple receive-diversity branches employing a linear Minimum-Mean-Square-Error (MMSE) receiver, which is the linear receiver that maximizes the SIR if noise is negligible compared to interference. The SIR is a useful metric in dense wireless networks which are interference-limited and directly influences achievable data rates if Gaussian transmit signals are assumed². The representative link is assumed to operate in a network with co-channel transmitters at correlated spatial positions. The asymptotic regime we consider is when the number of diversity branches N and potential transmitting nodes n (to be defined in Section II) go to infinity with a fixed positive ratio. We find that

This research was supported in part by the National Science Foundation under Grant CCF-1117218. Portions of this work were presented at the 2012 International Symposium on Information Theory (ISIT).

¹We use the term spatially correlated in this work to refer to networks where the *position* in space of randomly distributed transmitters is correlated, as compared to systems where *channel fading* between antennas are correlated

²Without the assumption of Gaussian transmit signals, we can apply a correction factor to the SIR to estimate the bits/symbol [6]. Moreover, since Gaussian interference maximizes the interference entropy, the bits/symbol computed by assuming Gaussian transmissions can be interpreted as a lower bound on the bits/symbol with non-Gaussian transmit signals.

an appropriately normalized version of the SIR, and under the assumption of Gaussian transmissions, the achievable bits/symbol converge in probability to deterministic quantities if the correlation between active transmitters satisfies an asymptotic independence property. The normalized mean bits/symbol is also found to converge to the same quantity. The asymptotic mean bits/symbol for different spatial correlation models that satisfy the asymptotic independence property, which includes independent transmissions, take a similar form, but with different effective densities of nodes. Thus, the asymptotic bits/symbol for systems with "large" numbers of diversity branches and correlated transmissions (satisfying the asymptotic independence property), is approximated well by the asymptotic bits/symbol for a network with independent transmissions but equivalent density of active nodes. This framework is applied to two hard-core models which are close analogs to the Matern type-I and type-II networks commonly used to model Carrier-Sense-Multiple-Access (CSMA) networks, cellular networks with frequency reuse, and a Boolean cluster model whereby nodes are active if they are within a certain distance of randomly distributed cluster center, which illustrates the applicability of this framework to a wide range of systems.

The majority of works which consider spatial correlation models which admit hard-core networks deal with systems that have no diversity (e.g. single antenna/node) and use asymptotic techniques or other approximations as hard-core networks are known to be particularly difficult to analyze [7]. For instance, Haenggi, in [7], analyzes Matern Type-I and II hard-core networks with single-antenna nodes by finding bounds on the mean interference. Ganti, Andrews and Haenggi in [8], and Giacomelli, Ganti and Haenggi in [9], analyze networks with single-antenna nodes at correlated positions (including hard-core networks) using asymptotic techniques. In particular they consider the high SIR and reliability regimes respectively, where the density of active nodes is taken to zero. The few prior works that consider multi-antenna systems in hard-core networks (e.g. [10]) approximate the positions of the active nodes by a non-homogenous Poisson process by reducing the density of active nodes in the vicinity of a test receiver, but assuming that node positions are uncorrelated. In contrast to these works, the hard-core models we analyze (which are close analogs to the Matern type-I and II systems) explicitly consider spatially correlated transmitting nodes, with receive diversity. The complexity caused by the spatial correlation of active nodes is handled by the asymptotic analysis.

The analysis of cellular networks with regular cells, even for the simpler case of universal frequency reuse, is known to be very difficult (as noted in [6] and [11]), and are usually analyzed by Monte-carlo simulation such as in [12] and other references given in [11]. In a recent work [13], we consider the uplink of a cellular system in a similar asymptotic regime but with the active nodes at independent locations on the plane. In contrast, the framework developed in this work is applicable to cellular networks which use orthogonal multiple-access, whereby at most one user is allowed to transmit in a given time slot per cell, and nearby-cells occupy different frequency bands according to some frequency reuse pattern, which results in spatially correlated transmitters.

Of the network models with correlated active users, clustered wireless networks have proven to be somewhat tractable compared to the hard-core networks and frequency-reuse systems discussed above. In particular, networks with Poisson clusters, whereby users are distributed independently in clusters, with the cluster centers forming a homogenous Poisson Point Process (PPP) on the plane have been analyzed in works such as [14] and [15]. The main feature of Poisson cluster processes that makes them amenable to analysis is the high degree of independence inherent in the model, since the locations of users within each cluster are independent. Furthermore, the cluster locations are independent as well. The framework we develop in this work however, is applicable to a different cluster model, namely the Boolean cluster model whereby nodes are distributed independently on the plane, and nodes are actively transmitting if they are within a certain distance of at least one cluster center. The cluster centers are distributed randomly and independently on the plane. A major difference between the Boolean cluster model and the Poisson cluster model is that in the former, the density of active nodes on the plane is either zero or a positive constant. In the Poisson cluster model however, the density of nodes on the plane could vary significantly as regions where $K > 1$ clusters overlap say, will have K times the density of nodes compared to regions of the plane where there is a single cluster.

The asymptotic analyses carried out in this work are validated by Monte Carlo simulations which show a close agreement between the asymptotic predictions (particularly the mean bits/symbol) and simulated values, even when the diversity order per receiver is only moderately large (e.g. 6). This finding is consistent with what has been frequently observed in the random matrix literature, whereby the convergence of various quantities to their asymptotic values are rapid. Note that while it would be ideal to have an exact statistical characterization of the Signal-to-Interference-plus-Noise Ratio (SINR) for finite systems with the forms of spatial correlations that fall under our framework, we note that such systems have proven extremely difficult to analyze exactly, even for single antenna systems, as noted in the references summarized above and evidenced by the approximations that are frequently used in the literature to analyze such networks. Thus, the asymptotic technique developed here can be used to gain insight into the performance of networks which are known to be very difficult to analyze, and for which few analytical results of any form exist in the literature.

II. SYSTEM MODEL

Consider a circular network of radius R centered at the origin, with a representative receiver at the origin. The representative receiver is in a link with a representative transmitter located at a deterministic point X_T which is at distance $r_T = |X_T|$ from the origin. The representative receiver has N diversity branches (e.g. antennas or frequency diversity), with independent flat fading on each diversity branch. In addition to the representative transmitter, there are n potential interferers in the network, which if active, are co-channel interferers to the representative link. We use the word potential here since some of the potential interferers will not be actively transmitting as described later in this section. Let the potential interferer locations be denoted X_1, X_2, \dots, X_n with the distance of the i -th potential interferer from the origin denoted by $r_i = |X_i|$. The n potential interferers are i.i.d. with uniform probability in the circular network such that the area density of potential interferers ρ_p satisfies

$$n = \pi \rho_p R^2. \quad (1)$$

The average power (averaged over the fading realizations) received at each diversity branch of the representative receiver from an transmitter at distance r_i , transmitting with power P_i is $p_i = P_i r_i^{-\alpha}$, with $\alpha > 2$. The transmit power of the i -th potential interferer, P_i equals one or zero, and the transmit power of the representative transmitter is fixed at unity. Therefore, the vector of transmit powers $\mathbf{p} = (P_1, P_2, \dots, P_n)$ controls which of the potential interferers are active, and the representative transmitter is assumed to always be active.

The vector \mathbf{y} defined as follows contains the sampled signals at a given sampling time at the N diversity branches of the representative receiver.

$$\mathbf{y} = r_T^{-\frac{\alpha}{2}} \mathbf{g}_T x_T + \sum_{i=1}^n r_i^{-\frac{\alpha}{2}} \mathbf{g}_i \sqrt{P_i} x_i + \mathbf{w}, \quad (2)$$

where x_i (x_T), is the transmitted symbol of potential interferer i (representative transmitter), and $\mathbf{g}_i \in \mathbb{C}^{N \times 1}$ ($\mathbf{g}_T \in \mathbb{C}^{N \times 1}$) contains i.i.d., zero-mean, unit variance random variables drawn from a continuous distribution, representing the fading between the i -th potential interferer (representative transmitter) and the N diversity branches of the representative receiver. $\mathbf{w} \in \mathbb{C}^{N \times 1}$ represents independent zero-mean, circularly-symmetric Gaussian noise of variance σ^2 per complex dimension. In this paper, we shall focus on the interference-limited regime and neglect the noise by setting $\sigma^2 = 0$. The active nodes in the network are assigned non-zero transmit powers by a function $g(\cdot)$ such that $\mathbf{p} = g(X_1, \dots, X_n; M_1, M_2, \dots, M_m; X_T)$. M_1, \dots, M_m are auxiliary random variables that are used to select the active transmitters and are defined differently according to the specific spatial correlation model. For instance, in the HC-II model these variables are used to select which node is active when there are two or more nodes within each others hard core, and in the Boolean cluster model, these variables represent the cluster centers. The function $g(\cdot)$, thus controls which of the n potential interferers are transmitting, and since it is parameterized by X_T ,

the transmit powers of the interferers are a function of the locations of all potential transmitters (potential interferers and the representative transmitter) in the network. We denote the set of active transmitters as $\mathcal{T} := \{i : P_i = 1\}$.

The asymptotic regime we shall consider is the limit as N , n and $R \rightarrow \infty$, such that $n/N = c > 0$ and ρ_p are constants, and (1) holds. For the rest of this paper, whenever any one of the quantities n , N or $R \rightarrow \infty$, it is assumed that the other two quantities go to infinity as well, such that $n/N = c$ and (1) hold. The main results are given in terms of limiting values of a normalized version of the SIR, $\beta_N = N^{-\alpha/2} r_T^\alpha \text{SIR}$, at the output of the MMSE receiver. This normalization is used because the (unnormalized) SIR grows with the number of diversity branches as $N^{\alpha/2}$. Thus, using the standard formula for the SIR at the output of an MMSE receiver, we have

$$\beta_N = N^{-\frac{\alpha}{2}} \mathbf{g}_T^\dagger \left(\sum_{i=1}^n P_i r_i^{-\alpha} \mathbf{g}_i \mathbf{g}_i^\dagger \right)^{-1} \mathbf{g}_T. \quad (3)$$

Define $p_{in} = N^{\alpha/2} P_i r_i^{-\alpha}$, and $p_{jn} = N^{\alpha/2} P_j r_j^{-\alpha}$ for convenience. The spatial correlation between the transmitting nodes needs to satisfy the following asymptotic independence property,

$$\lim_{n \rightarrow \infty} \frac{1}{n^2} \sum_{i=1}^n \sum_{j=1}^n [\Pr(p_{in} \leq x, p_{jn} \leq x) - \Pr(p_{in} \leq x) \Pr(p_{jn} \leq x)] = 0. \quad (4)$$

If there is symmetry between the indices of the potential interferers, i.e. $\Pr(p_{in} \leq x) = \Pr(p_{jn} \leq x) \forall i, j$ and for all $i \neq j$ and $k \neq \ell$, $\Pr(p_{in} \leq x, p_{jn} \leq x) = \Pr(p_{kn} \leq x, p_{\ell n} \leq x)$, then (4) directly simplifies to the following for $i \neq j$

$$\lim_{n \rightarrow \infty} \Pr(p_{in} \leq x, p_{jn} \leq x) = \lim_{n \rightarrow \infty} \Pr(p_{in} \leq x) \Pr(p_{jn} \leq x). \quad (5)$$

Note that p_{in} is the average received power (if averaged over the fading distribution) from node i scaled by $N^{\alpha/2}$, as observed at the origin. Furthermore, note that although we refer to (4) and (5) as asymptotic independence, it is a slightly weaker requirement than asymptotic independence as the joint CDFs and the product of the marginal CDFs of p_{in} and p_{jn} that appear in (4) and (5) are evaluated at a common argument x . The asymptotic independence property is of course trivially satisfied if the locations of the active nodes are independent. Additionally, define ν as the average probability of a potential interferer being active in the limit, given by

$$\nu = \lim_{n \rightarrow \infty} \frac{1}{n} \sum_{i=1}^n \Pr(P_i = 1). \quad (6)$$

We require that $\nu/N > 1$, in other words, there are more active interferers than the diversity order at the receiver in the limit.

III. MAIN RESULT

The empirical distribution function (e.d.f.) of a set of random variables, which is used in the main results, is defined as the proportion of those random variables that are less than or equal to the argument of the e.d.f. For instance, denoting the e.d.f. of p_{in} by $H_n(x)$, we have

$$H_n(x) = \frac{1}{n} \sum_{i=1}^n 1_{\{p_{in} \leq x\}} = \frac{1}{n} \sum_{i=1}^n a_{in}(x), \quad (7)$$

where $1_{\{\cdot\}}$ is the indicator function, and $a_{in}(x) = 1_{\{p_{in} \leq x\}}$. We can now state the main result.

Theorem 1: If the asymptotic independence property defined in (4) holds, as $n, N, R \rightarrow \infty$ such that $n/N = c > 0$, and (1) hold, $\beta_N \rightarrow \beta$ in probability where β is the real, positive solution to

$$1 = \beta c \int_0^\infty \frac{\tau dH(\tau)}{1 + \tau \beta}, \quad (8)$$

where $H(x)$ is defined as follows

$$\lim_{n \rightarrow \infty} H_n(x) \rightarrow H(x), \text{ in probability.} \quad (9)$$

The convergence in probability above is guaranteed by (4). Additionally, if the following holds,

$$\lim_{n \rightarrow \infty} \Pr(r_i^{-\alpha} N^{\frac{\alpha}{2}} \leq x | P_i = 1) = \lim_{n \rightarrow \infty} \Pr(r_i^{-\alpha} N^{\frac{\alpha}{2}} \leq x), \quad (10)$$

then (8) evaluates to

$$\frac{2\pi^2 \rho \beta^{\frac{2}{\alpha}}}{\alpha} \csc\left(\frac{2\pi}{\alpha}\right) = 1 + \frac{2(\pi\rho)^{2-\frac{2}{\alpha}}\beta}{(\alpha-2)(c+\pi\rho\beta)^{1-\frac{2}{\alpha}}} {}_2F_1\left(1-\frac{2}{\alpha}, 1-\frac{2}{\alpha}; 2-\frac{2}{\alpha}; \frac{\pi\rho\beta}{\pi\rho\beta+c}\right). \quad (11)$$

where $\rho = \rho_p \nu$, and ${}_2F_1(\cdot, \cdot; \cdot; \cdot)$ is the Gauss hypergeometric function (e.g. see [16]).

Proof: Given in Appendix A.

Note that ρ is the effective density of active transmissions in the limit. Additionally, note that when the N is large, the SIR is not strongly influenced by the dependence of the transmit powers as β is only dependent on the marginal probability that a node is selected to transmit. This leads to simple approximations to the bits/symbol given later in this section as the complicated dependence between transmit powers becomes negligible with large N .

If we assume that the locations of the potential interferers are independent, then the asymptotic independence property is trivially satisfied, which means Theorem 1 holds. Hence, the normalized SIR in systems with correlated active transmitters, (but satisfying the asymptotic independence property), converges to the same limit as a network with independent transmitters with equal density of transmitting nodes.

Assuming that all nodes use Gaussian code books and recalling that the thermal noise is negligible, we estimate the bits/symbol using the Shannon formula, $C_N = \log_2(1 + \text{SIR})$, where the subscript N is used to emphasize the dependence of the bits/symbol on the number of receiver degrees of freedom. By the continuity of the log function,

$$|\log_2(1 + \text{SIR}) - \log_2(1 + r_T^{-\alpha} N^{\frac{\alpha}{2}} \beta)| \rightarrow 0$$

in probability as $N \rightarrow \infty$ in the manner of Theorem 1. Furthermore, applying the bounded convergence theorem in the manner of [17], we can show that

$$E[\log_2(1 + \text{SIR})] - \log_2(1 + r_T^{-\alpha} N^{\frac{\alpha}{2}} \beta) \rightarrow 0.$$

Hence, $\log_2(1 + r_T^{-\alpha} N^{\frac{\alpha}{2}} \beta)$ is a good approximation for the mean bits/symbol when the diversity order N is large.

In general, the solution for β in (8) or (11) has to be found numerically. However, if (10) holds, and the diversity order at the receiver N is much smaller than the number of potential interferers in the network n , c is large, and we can find a simple approximation for β that exposes the dependency of the SIR on system parameters. Note that the hypergeometric function in the second term on the RHS of (11) has positive parameters implying that it is a power series with positive coefficients. Hence, the second term on the RHS of (11) is non-negative and is an increasing function of its argument, and thus is bounded from above by

$$\frac{2(\pi\rho)^{2-\frac{2}{\alpha}}\beta}{(\alpha-2)(c+\pi\rho\beta)^{1-\frac{2}{\alpha}}} {}_2F_1\left(1-\frac{2}{\alpha}, 1-\frac{2}{\alpha}; 2-\frac{2}{\alpha}; 1\right) = \frac{2\pi(\pi\rho)^{2-\frac{2}{\alpha}}\beta}{\alpha(c+\pi\rho\beta)^{1-\frac{2}{\alpha}}} \csc\left(\frac{2\pi}{\alpha}\right) \quad (12)$$

Since $\alpha > 2$, as $c \rightarrow \infty$, the previous expression goes to zero. Thus the second term on the RHS of (11) goes to zero as well. Thus, if the number of potential interferers in the network n , greatly exceeds the

diversity order at the receiver, i.e. c is very large, the second term on the RHS of (11) is small and β can be approximated as

$$\beta \approx \left[\frac{\alpha}{2\pi^2\rho} \sin\left(\frac{2\pi}{\alpha}\right) \right]^{\frac{\alpha}{2}}. \quad (13)$$

Thus, when N and n are both large but $n \gg N$, the normalized SIR β_N can be approximated by β . Removing the normalization by $N^{\alpha/2}$ and applying the Shannon formula leads to the following approximation for the bits/symbol and its mean

$$C \approx E[C] \approx \log_2 \left(1 + \left[N \frac{\alpha}{2\pi^2\rho r_T^2} \sin\left(\frac{2\pi}{\alpha}\right) \right]^{\frac{\alpha}{2}} \right). \quad (14)$$

IV. APPLICATION TO MATERN-LIKE HARD CORE MODELS

We apply the framework developed in Section III to two hard-core models, HC-I and HC-II which are analogous to the Matern Type I and II models commonly used to model hard-core processes [18]. Hard-core models are simple models for active nodes in systems with MAC protocols where nodes that are close to each other are not allowed to transmit simultaneously. For instance, the Matern Type II model has been used to model CSMA networks [19] in which nodes are not allowed to transmit if they detect an ongoing transmission in their vicinity.

In the HC-I model we assume that all n interferers in the radius R network are active unless they are within a distance h of any other interferer or the representative transmitter. In the HC-II model, each interferer is assigned an independent uniform $(0, 1]$ random variable called a mark, where the mark assigned to the i -th interferer is M_i . All interferers are active unless they are within a distance h of the representative transmitter, or if they are within a distance h of any potential interferer *and* have a higher mark than that potential interferer.

In comparison, the Matern type I and type II processes are constructed from an underlying Poisson point processes. For the Type I process, each point of the underlying Poisson process that is within a distance h from another point of the underlying process is removed. For the Type II process, a point of the underlying Poisson process is retained only if there is no other point of the Poisson process within a distance h of it which has a mark of lesser value. Thus, these processes are the result of dependent thinning of an underlying Poisson point process. To incorporate an active transmitter at a particular location, the Matern process has to be conditioned on having a node at that location which leads to added mathematical complexity as the probability of a node being at a particular point is zero. We sidestep this complexity for HC-I and HC-II by assuming that the representative transmitter is not part of the random process but is located at a deterministic point.

Recall that $(P_1, P_2, \dots, P_n) = g(X_1, X_2, \dots, X_n; M_1, M_2, \dots, M_n; X_T)$ assigns the transmit powers to the interferers and can be defined as follows. For the HC-I model,

$$P_i = \begin{cases} 0 & \text{if } |X_i - X_T| < h \text{ or } \exists j \text{ such that } |X_i - X_j| < h \\ 1 & \text{otherwise.} \end{cases} \quad (15)$$

For the HC-II model,

$$P_i = \begin{cases} 0 & \text{if } |X_i - X_T| < h \text{ or } \exists j \text{ such that } |X_i - X_j| < h \text{ and } M_i > M_j \\ 1 & \text{otherwise.} \end{cases} \quad (16)$$

The HC-I and HC-II models satisfy the asymptotic independence property in (5), and (10), as shown in Appendix D. Thus, (14) can be used to approximate the asymptotic and mean bits/symbol for these models with the appropriate limiting effective density of transmissions ρ . The limiting values of ρ are derived in Appendix D and are as follows.

For the HC-I model, as $R \rightarrow \infty$,

$$\rho = \rho_p \Pr(P_i = 1) \rightarrow \rho_p \exp(-\rho_p \pi h^2). \quad (17)$$

For the HC-II model, as $R \rightarrow \infty$,

$$\rho \rightarrow \frac{1}{\pi h^2} (1 - \exp(-\rho_p \pi h^2)). \quad (18)$$

V. FREQUENCY REUSE SYSTEMS

In certain wireless communications systems such as cellular networks with Time-Division-Multiple-Access (TDMA) and frequency reuse, at most one wireless node is allowed to transmit at a given time, in a given frequency band, and in a given spatial region. The active nodes in such a network are of course spatially correlated and the framework developed above can be used to analyze such systems. Note that cellular systems with regular cells are notoriously difficult to analyze in closed form, even when there is universal frequency reuse, as noted in references such as [20]. Thus, the asymptotic analysis provided here provides insight into a problem that is known to be challenging.

Consider the network illustrated in Figure 1 which shows a cellular network with reuse factor 3, with only one transmitter active in a given time slot, in a given cell. The base stations are represented by the dots and the representative transmitter by the square and the in-band transmitters by the crosses.

To apply the framework developed above, we first assume that the base stations are distributed on a plane in a hexagonal grid pattern, with one base station (the representative receiver) located at the origin. Let ρ_c denote the area density of the base stations. The representative transmitter is located at a deterministic point in the cell at the origin. Overlaid on this grid of base stations is the circular network of radius R , centered at the origin with n potential interferers distributed in an i.i.d. fashion, with uniform probability in the circular network with their positions denoted as X_1, X_2, \dots, X_n as in Section III. As in the HC-II model, we assign each potential interferer a mark which is an i.i.d. random variable uniformly distributed on $(0,1]$. The mark associated with the i -th potential interferer is denoted by M_i , and is used to decide which node transmits in a given cell. Let us assume that the cell at the origin, denoted \mathcal{C}_0 , is assigned to frequency band 0, and the other cells assigned to band 0 be denoted $\mathcal{C}_1, \mathcal{C}_2, \dots$. For simplicity, we shall not consider power control in this work (systems which employ power control, and more general cell and reuse structures will be treated in a future work). The set of active nodes in band 0 in a given time slot is determined by the function $g(X_1, X_2, \dots, X_n; M_1, M_2, \dots, M_m; X_T)$ defined as follows.

$$P_i = \begin{cases} 1 & \text{if } \exists j \text{ s.t. } X_i \in \mathcal{C}_j \text{ AND } M_i < M_k \forall k \neq i \text{ for which } X_k \in \mathcal{C}_j \\ 0 & \text{otherwise} \end{cases} \quad (19)$$

As shown in Appendix G, this model satisfies the asymptotic independence property in (5), and (10). The limiting effective density ρ is found in Appendix G to be

$$\rho = \frac{1}{\kappa} \rho_c \left(1 - e^{-\frac{\rho_p}{\rho_c}} \right). \quad (20)$$

Thus, we can approximate the mean bits/symbol of link with length r_T by (14) and ρ as above. The reuse factor (3 in the example) is denoted by κ . Note that if the representative transmitter is located at the cell edge, $\rho_c = \frac{2}{\sqrt{3}r_T^2}$. Substituting for ρ_c in (20) and the resulting expression for ρ into (14) yields the following expression for the mean spectral efficiency of a cell-edge user

$$E[C] \approx \log_2 \left(1 + \left[N \frac{\kappa \alpha}{2\pi^2 \left(1 - e^{-\frac{\rho_p}{\rho_c}} \right)} \sin \left(\frac{2\pi}{\alpha} \right) \right]^{\frac{\alpha}{2}} \right). \quad (21)$$

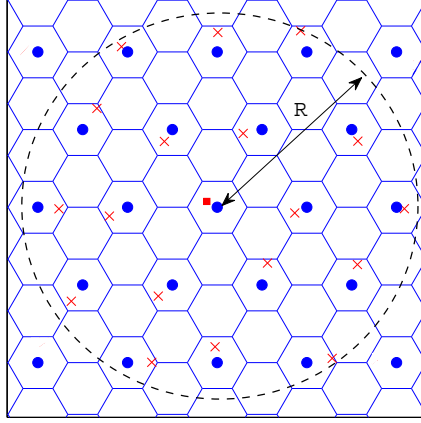


Fig. 1. Illustration of a cellular network with frequency reuse of 3. Active mobile nodes in a given time slot at a given frequency band are illustrated by the crosses. The representative transmitter is assumed to transmit in the given time-slot and frequency band and is denoted by the square, and the base stations are denoted by the dots. The mobile users (both active and inactive) are distributed randomly with uniform probability in the circular network of radius R which is then taken to infinity

When the density of potential interferers to base stations is high, (21) further simplifies to

$$E[C] \approx \log_2 \left(1 + \left[N \frac{\kappa \alpha}{2\pi^2} \sin \left(\frac{2\pi}{\alpha} \right) \right]^{\frac{\alpha}{2}} \right). \quad (22)$$

Note that the last expression takes a very simple form which depends only on a few parameters. Its accuracy over reasonable values of N , α and other parameters is validated in Section VII.

VI. BOOLEAN CLUSTER NETWORKS

In this section, we illustrate the utility of Theorem 1 to the Boolean cluster model which is described in Section I, which also details how it differs from the related Matern cluster model. More precisely, we can define the Boolean cluster model as follows.

Consider a set of cluster centers M_1, M_2, \dots, M_m , i.i.d., with uniform probability, in the circular network such that $m = \pi \rho_b R^2$, where ρ_b is the density of the boolean clusters. The function $g(X_1, X_2, \dots, X_n; M_1, M_2, \dots, M_m)$ for this model can be written as follows.

$$P_i = \begin{cases} 1 & \text{if } X_i \in \bigcup_{i=1}^m B(M_i, h) \\ 0 & \text{otherwise,} \end{cases} \quad (23)$$

where $B(X, d)$ is a disk of radius d centered on X . Note that this model trivially satisfies the asymptotic independence property because as $R \rightarrow \infty$, the probability that two potential interferers X_i and X_j same cluster diminishes to zero, making their transmit powers independent asymptotically. The effective density of active transmissions is given simply by the product of the density of potential interferers ρ_p and the percent coverage of the Boolean model (see e.g. [18]) with circular grains of radius h . This value is

$$\rho = \rho_p \left(1 - e^{-\rho_b \pi h^2} \right). \quad (24)$$

Thus, the mean spectral efficiency is given by (14) with the above definition for the limiting effective density of interferers.

VII. NUMERICAL SIMULATIONS

We conducted Monte Carlo simulations to validate the asymptotic results for the mean bits/symbol derived in the previous sections, for the different systems considered in this paper.

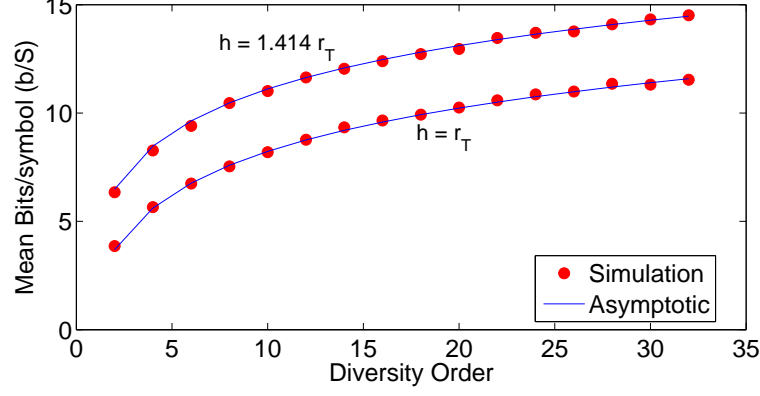


Fig. 2. Mean bits/symbol with the HC-I model of interferers. The link length r_T was such that $\pi\rho pr_T^2 = 1$, and the radius of the guard zone, h was a multiple of r_T as labeled in the figure.

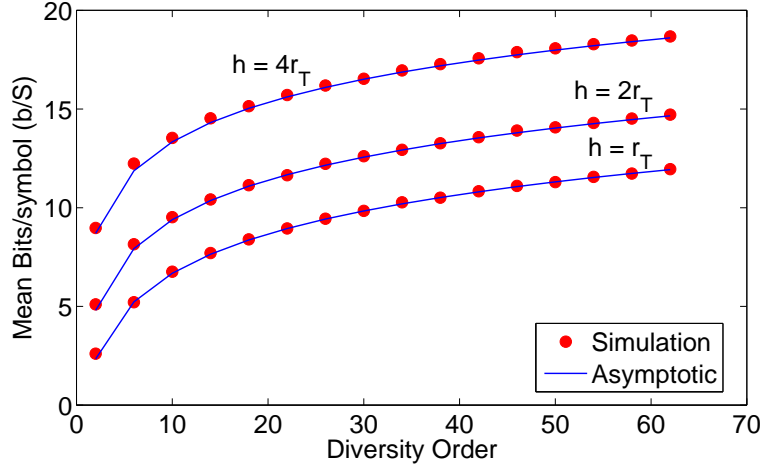


Fig. 3. Mean bits/symbol with HC-II model of interferers. The link length r_T was such that $\pi\rho pr_T^2 = 1$, and the radius of the guard zone, h was a multiple of r_T as labeled in the figure.

A. Maternlike hard-core models

We simulated both HC-I and HC-II networks with $\alpha = 4$. The link-lengths r_T for both sets of simulations were selected such that $\pi\rho pr_T^2 = 1$, i.e. on average 1 other potential interferer is closer to the representative receiver than the representative transmitter. The radius of the guard zones h were varied as a function of r_T and are given in the corresponding figures.

Figure 2 illustrates the mean bits/symbol from 1000 simulations of the HC-I model with guard zones that are a multiple of the length of the representative link. Note from the figure that the asymptotic approximation is very close to the simulated mean bits/symbol. For $N \geq 6$ diversity branches, the simulated and asymptotic mean bits/symbol (from (14)) with ρ defined appropriately) are virtually indistinguishable. Figure 3 illustrates the mean bits/symbol from simulations of the HC-II model with guard zones that are a multiple of the length of the representative link. Note from the figure that the asymptotic approximation is very close to the simulated mean bits/symbol, even when the number of diversity branches is small. Figure 4 shows the bits/symbol obtained from 100 simulations of the HC-II process for different receive diversity orders. The concentration of points with increasing diversity order indicates that the bits/symbol concentrates on the asymptotic prediction which implies convergence in probability.

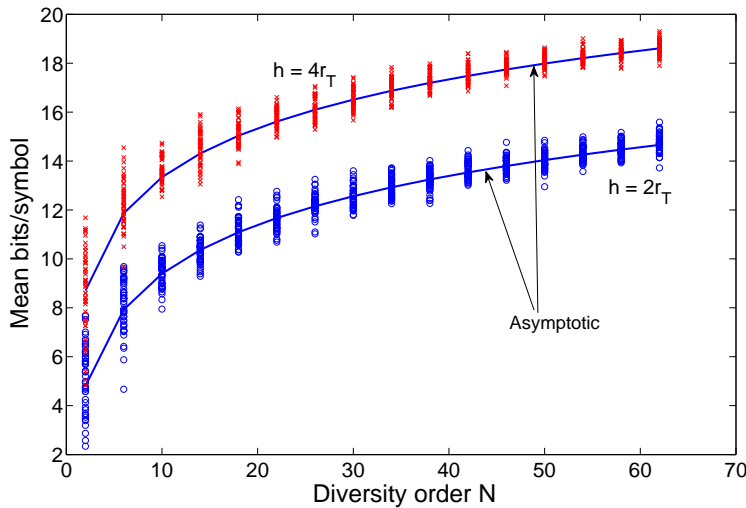


Fig. 4. Bits/symbol from 100 simulations of HC-II model of interferers vs. receive diversity order. The link length r_T was such that $\pi\rho_p r_T^2 = 1$, and the radius of the guard zone, h was a multiple of r_T as labeled in the figure.

B. Frequency-reuse Systems

In order to validate the asymptotic results presented in Section V, we simulated cellular networks with hexagonal cells and frequency reuse factor 3 as illustrated in Figure 1. The path-loss exponent $\alpha = 4$, the density of potential interferers (wireless nodes) $\rho_p = 0.01$ and different relative densities of base stations to wireless nodes (indicated in the Figure) were used. At most one node was allowed to transmit in any active cell. Figure 5 illustrates the mean bits/symbol of the representative link of length r_T , where r_T was such that $\pi\rho_p r_T^2 = 1$, i.e. there is on average one potential interferer closer to the representative base station than the representative transmitter.

The markers in Figure 5 illustrate the simulated values and the solid lines represent (14), with the effective density of interferers ρ given by (20). The asymptotic prediction for the mean spectral efficiencies are within 1% of the simulated values for $N \geq 6$, validating the asymptotic predictions. The dashed lines represent the simulated standard deviations which decay with diversity order. For the systems we simulated, the standard deviation is less than 5% of the asymptotic predictions when $N \geq 10$. The decaying standard deviation indicates mean-square convergence which implies convergence in probability.

Figure 6 represents simulations of a similar network model with $\rho_c/\rho_p = 0.05$, with the representative transmitter located at the edge of the cell centered at the origin. The figure shows the reuse-normalized mean bits/symbol vs. the diversity order at the representative base station, i.e. the vertical axis of the graph illustrates $\frac{1}{3}$ times the mean bits per symbol. The simulated values agree with the asymptotic prediction to within 1.05 % when the diversity order is six or greater. We also plotted the asymptotic mean bits/second for a system with universal frequency reuse on the same graph (dashed line) which illustrates that a several fold increase in mean bits/symbol (normalized by reuse factor) is possible by implementing frequency reuse, even when the system is interference limited as is assumed throughout this work.

C. Boolean Cluster Model

In order to validate the asymptotic results presented in Section VI, we simulated Boolean cluster networks with path-loss exponent $\alpha = 4$. The density of potential interferers (wireless nodes) $\rho_p = 0.01$ and different relative densities of clusters to wireless nodes was used. Figure 7 illustrates the mean bits/symbol of the representative link of length r_T . r_T was such that $\pi\rho_p r_T^2 = 1$, i.e. there is on average one node closer to the representative base station than the representative transmitter. The simulated mean bits/symbol are represented by the markers and the asymptotic prediction of (14) with the effective density

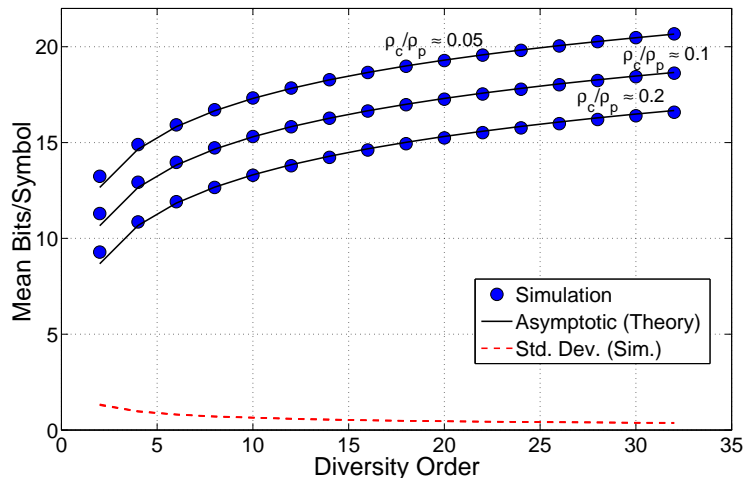


Fig. 5. Mean bits/symbol vs. receiver diversity order for cellular system with reuse factor of 3 and different relative densities of wireless nodes to base stations. Representative link length r_T is such that $\pi\rho_p r_T^2 = 1$. The three dashed lines (difficult to distinguish on this scale) represent the decaying standard deviation of the bits/symbol.

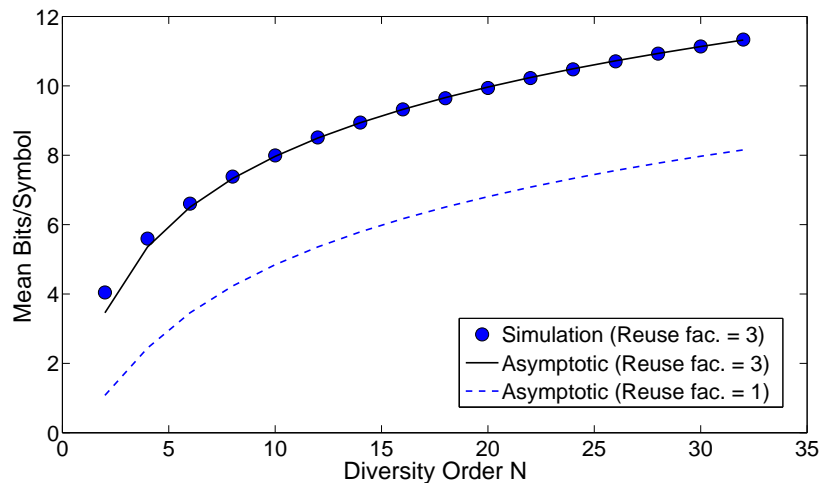


Fig. 6. Mean bits/symbol normalized by reuse factor vs. receiver diversity order for cellular system with reuse factor of 3 and relative density of base stations to wireless nodes $\rho_c/\rho_p = 0.05$. The representative transmitter is located at the edge of the cell. To illustrate, the asymptotic mean bits/symbol for a universal frequency reuse system is also plotted.

of active interferers given by (24) is represented by the solid line. The simulated mean bits/symbol agrees with the asymptotic expression to within 2.5% when the number of diversity branches is 8 or larger in all the cases we considered. The dashed lines in the figure indicate the standard deviation of the bits/symbol from simulations which decay with increasing diversity order. For the cases we consider, the standard deviation is 10% or less of the asymptotic prediction when the number of diversity branches is 12 or more. The decay in standard deviation indicates convergence in mean square, and hence in probability.

VIII. SUMMARY AND CONCLUSIONS

An asymptotic technique to compute the mean bits/symbol achievable in wireless networks where active interferers are spatially correlated and receivers have N diversity branches with linear MMSE processing is introduced. In particular, we consider networks which are the result of the dependent thinning of an underlying process with independent node positions. The thinning operation is such that the received powers of pairs of nodes satisfy a particular asymptotic independence criteria. This framework is applied

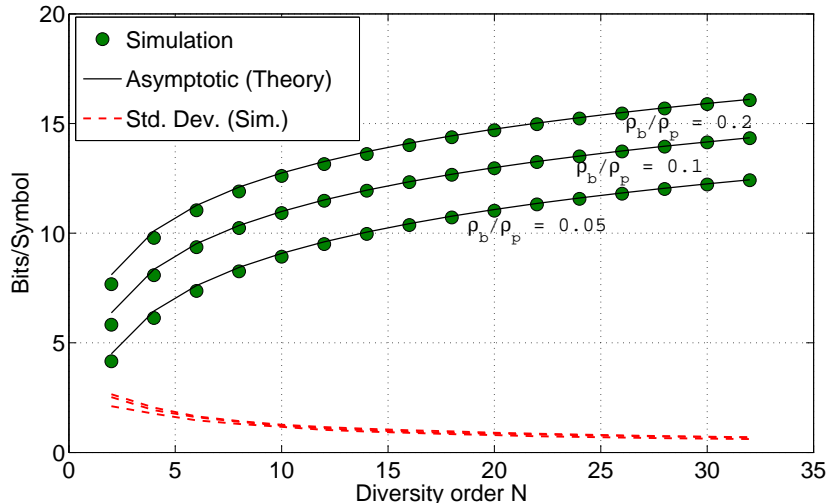


Fig. 7. Mean bits/symbol vs. diversity order for Boolean cluster model with varying cluster density. The three dashed lines represent the decaying standard deviation of the bits/symbol.

to two hard-core models, the HC-I and HC-II models defined in Section IV, which are analogous to Matern type I and II models which are frequently used to model networks with CSMA MAC protocols. We additionally apply this result to analyze cellular networks with orthogonal transmissions and frequency reuse patterns, and a Boolean cluster model which can be used to model networks with hotspots. These models, in particular the hard-core and cellular models have proven difficult to analyze in the literature.

For systems satisfying our model, when the receive diversity order N grows large, the influence of the spatial dependence of the active nodes on the bits/symbol diminishes. As a result, the mean bits/symbol for "large" N can be accurately approximated using simple expressions. These results provide insight into the benefits of increasing diversity order, which is directly related to cost in many systems, on the expected data rate. These results can also be utilized to optimize parameters such as the guard zone-radius in hard-core networks, and reuse factors in cellular systems to maximize mean data rates. The asymptotic results are validated by Monte carlo simulations which match theoretical predictions even when the diversity order is only moderately large. These findings provide insight into wireless networks with correlated transmissions, which are well known to be challenging to analyze, and for which only a limited number of analytical results exist in the literature.

APPENDIX

A. Proof of Main Result

The main property used in proving Theorem 1 is the following lemma which is a variant of Lemma 1 from Govindasamy et al. [13] and Lemma 4.3 of Tse and Hanly [21].

Lemma 1: Consider the quantity

$$\gamma_N = \frac{1}{N} \mathbf{s}^\dagger \left(\frac{1}{N} \mathbf{S} \mathbf{\Psi} \mathbf{S}^\dagger \right)^{-1} \mathbf{s} \quad (25)$$

where $\mathbf{s} \in \mathbb{C}^{N \times 1}$ and $\mathbf{S} \in \mathbb{C}^{N \times n}$ comprise i.i.d., zero-mean, unit-variance entries, $n/N = c$, and $\mathbf{\Psi} = \text{diag}(\psi_1, \psi_2, \dots, \psi_n)$. Suppose that as $n, N \rightarrow \infty$, the e.d.f. of $(\psi_1, \psi_2, \dots, \psi_n)$ converges in probability to $H(x)$. Additionally, assume that there exists an n_0 such that $\forall n > n_0, \lambda_{\min}(\frac{1}{N} \mathbf{S} \mathbf{\Psi} \mathbf{S}^\dagger) > \lambda_{\ell b} > 0$, with probability 1, where $\lambda_{\min}(\mathbf{A})$ denotes the minimum eigenvalue of \mathbf{A} . Then, $\gamma_N \rightarrow \gamma$ in probability where γ equals the non-negative real solution for β in (8).

Proof: By assumption, the e.d.f. of the diagonal entries of $\mathbf{\Psi}$ converges to a non-random limit in probability. Hence, by Theorem 4.1 of Bai and Silverstein [22], the e.d.f of the eigenvalues of $\frac{1}{N} \mathbf{S} \mathbf{\Psi} \mathbf{S}^\dagger$

converges in probability to a non-random limit. From Lemma 4.3 of [21] and Lemma 1 of [13], it is evident that Lemma 1 holds if the e.d.f. of the eigenvalues of $\frac{1}{N}\mathbf{S}\Psi\mathbf{S}^\dagger$ converges in probability to a non-random limit as $n, N \rightarrow \infty$. ■

Up to a scale factor, (25) has the same form as the equation for the normalized SIR β_N in (3) with $\mathbf{s} = \mathbf{g}_T$, $\Psi = \text{diag}(N^{\alpha/2}P_1r_1^{-\alpha}, N^{\alpha/2}P_2r_2^{-\alpha}, \dots, N^{\alpha/2}P_nr_n^{-\alpha})$, and $\mathbf{S} = [\mathbf{g}_1 \mathbf{g}_2 \dots \mathbf{g}_n]$. To use this result to characterize β_N , we first condition on the event (denoted by \mathcal{D}) that the fraction of potential interferers that are active is greater than $\frac{3}{4}$ of its limiting value. This conditioning assures that the minimum eigenvalue condition required in the lemma is satisfied. Note that the number $\frac{3}{4}$ here is somewhat arbitrary as any positive rational number less than one would suffice. Thus, \mathcal{D} is the event that $\frac{|\mathcal{T}|}{n} \geq \frac{3\nu}{4}$. Since $\frac{|\mathcal{T}|}{n} \rightarrow \nu$ in probability by the asymptotic independence property, as $n, N, R \rightarrow \infty$, $\Pr\left(\left|\frac{|\mathcal{T}|}{n} - \nu\right| > \frac{\nu}{4}\right) \rightarrow 0$, which implies that

$$\Pr(\mathcal{D}) = \Pr\left(\frac{|\mathcal{T}|}{n} \geq \frac{3\nu}{4}\right) \rightarrow 1. \quad (26)$$

We shall use this fact to remove the conditioning on \mathcal{D} .

To use Lemma 1, we first show that conditioned on \mathcal{D} , the e.d.f. of the $p_{in} = N^{\alpha/2}P_ir_i^{-\alpha}$ terms, defined in (7), converges in probability to a limiting function $H(x)$ in Lemma 2. We then show that the minimum eigenvalue property is satisfied in Lemma 3. The proof is completed by evaluating (8) with $H(x)$ from (28) in Lemma 2.

Lemma 2: If (4) holds and conditioned on \mathcal{D} , as $n, N, R \rightarrow \infty$ as in Theorem 1,

$$H_n(x) \rightarrow H(x) = \lim_{n \rightarrow \infty} \frac{1}{n} \sum_{i=1}^n \Pr(P_i = 1) \Pr(N^{\frac{\alpha}{2}}r_i^{-\alpha} < x | P_i = 1) + \frac{1}{n} \sum_{i=1}^n \Pr(P_i = 0), \quad (27)$$

where the convergence is in probability. If (10) holds, then

$$H(x) = 1 - \frac{\pi\rho}{c}x^{-\frac{2}{\alpha}}1\left\{\left(\frac{\pi\rho p}{c}\right)^{\alpha/2} < x\right\}. \quad (28)$$

Proof: Given in Appendix B

Lemma 3: Let Ψ and \mathbf{S} be as defined above. Conditioned on \mathcal{D} there exists an n_0 such that for all $n > n_0$, and with probability 1,

$$\lambda_{\min}\left(\frac{1}{N}\mathbf{S}\Psi\mathbf{S}^\dagger\right) = \lambda_{\min}\left(\frac{1}{N}\sum_{i=1}^n N^{\alpha/2}r_i^{-\alpha}P_i\mathbf{g}_i\mathbf{g}_i^\dagger\right) > \left(\frac{\pi\rho p}{c}\right)^{\frac{\alpha}{2}}\frac{3c\nu}{8}\left(1 - \sqrt{\frac{4}{3c\nu}}\right)^2. \quad (29)$$

Proof: Given in Appendix C

Thus, from Lemmas 1, 2 and 3, conditioned on \mathcal{D} , $\beta_N \rightarrow \beta$ in probability, i.e. for any $\epsilon > 0$

$$\Pr(|\beta_N - \beta| > \epsilon | \mathcal{D}) \rightarrow 0. \quad (30)$$

We remove the conditioning by using (30) and (26) as follows. For any $\epsilon > 0$,

$$\Pr(|\beta_N - \beta| > \epsilon) = \Pr(|\beta_N - \beta| > \epsilon | \mathcal{D}) \Pr(\mathcal{D}) + \Pr(|\beta_N - \beta| > \epsilon | \mathcal{D}^c) \Pr(\mathcal{D}^c) \rightarrow 0. \quad (31)$$

The first part of Theorem 1 is thus proved. If (10) holds, we can substitute the derivative of $H(x)$ from (28), into (8), and integrate to get

$$\frac{2\pi^2\rho\beta^{\frac{2}{\alpha}}}{\alpha}\csc\left(\frac{2\pi}{\alpha}\right) - \frac{2(\pi\rho)^{2-\frac{2}{\alpha}}\beta}{(\alpha-2)c^{1-\frac{2}{\alpha}}}{}_2F_1\left(1, 1 - \frac{2}{\alpha}, 2 - \frac{2}{\alpha}; -\frac{\pi\rho\beta}{c}\right) = 1 \quad (32)$$

This integral (without the scale factor of $\lim_{n \rightarrow \infty} \Pr(P_i = 1)$) has been evaluated before in [17], and we refer the reader there for the details of its computation. Applying the Pfaff transform (see e.g. [16]) to the hypergeometric function in (32) yields (11).

B. Proof of Lemma 2

We first will show that this property holds without the conditioning. Recalling the definition of $a_{in}(x)$ from Section III, note that $E[a_{in}(x)] = \Pr(p_{in} \leq x)$ and $E[a_{in}(x)a_{jn}(x)] = \Pr(p_{in} \leq x, p_{jn} \leq x)$. Next, define the following

$$\bar{H}_n(x) = \frac{1}{n} \sum_{i=1}^n E[a_{in}(x)] = \frac{1}{n} \sum_{i=1}^n \Pr(r_i^{-\alpha} P_i N^{\alpha/2} \leq x) \quad (33)$$

$$\bar{H}_\infty(x) = \lim_{n \rightarrow \infty} \bar{H}_n(x) \quad (34)$$

Recall the definition of $H_n(x)$ from Section III. Since (34) converges, for each $\epsilon > 0$, $\exists n_a$ such that for all $n > n_a$, $|\bar{H}_n(x) - \bar{H}_\infty(x)| \leq \frac{1}{2}\epsilon$. Thus $\forall n > n_a$,

$$\begin{aligned} \Pr(|H_n(x) - \bar{H}_\infty(x)| > \epsilon) &\leq \Pr(|H_n(x) - \bar{H}_n(x)| > \frac{\epsilon}{2}) \\ &= \Pr\left(\left|\sum_{i=1}^n a_{in}(x) - \sum_{i=1}^n E[a_{in}(x)]\right| > \frac{n\epsilon}{2}\right) \leq \frac{4}{\epsilon^2 n^2} \text{var}\left\{\sum_{i=1}^n a_{in}(x)\right\} \\ &= \frac{4}{\epsilon^2 n^2} \sum_{i=1}^n \sum_{j=1}^n \text{cov}(a_{in}(x), a_{jn}(x)) = \frac{4}{\epsilon^2 n^2} \sum_{i=1}^n \sum_{j=1}^n (E[a_{in}(x)a_{jn}(x)] - E[a_{in}(x)]E[a_{jn}(x)]) \\ &= \frac{4}{\epsilon^2 n^2} \sum_{i=1}^n \sum_{j=1}^n (\Pr(p_{in} \leq x, p_{jn} \leq x) - \Pr(p_{in} \leq x)\Pr(p_{jn} \leq x)) \end{aligned} \quad (35)$$

where the inequality follows from the Chebyshev inequality. As $n, N, R \rightarrow \infty$, from (4) we have (35) going to zero. Now, if we let

$$H(x) = \bar{H}_\infty(x), \quad (36)$$

$\Pr(|H_n(x) - H(x)| > \epsilon) \rightarrow 0$ which implies that $H_n(x)$ converges in probability to $H(x)$. Now since \mathcal{D} holds with probability approaching unity, we have

$$\begin{aligned} \Pr(|H_n(x) - H(x)| > \epsilon | \mathcal{D}) &= \frac{1}{\Pr(\mathcal{D})} [\Pr(|H_n(x) - H(x)| > \epsilon) - \\ &\Pr(|H_n(x) - H(x)| > \epsilon | \mathcal{D}^c) \Pr(\mathcal{D}^c)] \rightarrow 0 \end{aligned} \quad (37)$$

To show (27), we note from (33), (36), that as $n, N, R \rightarrow \infty$,

$$H(x) \rightarrow \frac{1}{n} \sum_{i=1}^n [\Pr(P_i N^{\frac{\alpha}{2}} r_i^{-\alpha} \leq x | P_i = 1) \Pr(P_i = 1) + \Pr(P_i N^{\frac{\alpha}{2}} r_i^{-\alpha} \leq x | P_i = 0) \Pr(P_i = 0)]$$

which implies (27) since $\Pr(P_i N^{\frac{\alpha}{2}} r_i^{-\alpha} \leq x | P_i = 0) = 1$.

For each n , the r_i 's are identically distributed. Thus, if (10) holds, (27) becomes

$$H(x) = \lim_{n \rightarrow \infty} \frac{1}{n} \sum_{i=1}^n \Pr(P_i = 1) \Pr(N^{\frac{\alpha}{2}} r_1^{-\alpha} \leq x) + \lim_{n \rightarrow \infty} \frac{1}{n} \sum_{i=1}^n \Pr(P_i = 0) \quad (38)$$

Additionally, we note from [1] that the CDF of $N^{\alpha/2} r_1^{-\alpha}$ is

$$\Pr(N^{\alpha/2} r_1^{-\alpha} \leq x) = 1 - \frac{\pi \rho_p}{c} x^{-\frac{2}{\alpha}} 1_{\left\{\left(\frac{\pi \rho_p}{c}\right)^{\alpha/2} < x\right\}}, \quad (39)$$

which does not depend on N because N , n , and R are related such that the CDF of $N^{\alpha/2}r_1^{-\alpha}$ is independent of N . Substituting (39) into (38) yields the following as $N, n, R \rightarrow \infty$,

$$H(x) = \left(\lim_{n \rightarrow \infty} \frac{1}{n} \sum_{i=1}^n \Pr(P_i = 1) \right) \left(1 - \frac{\pi \rho_p}{c} x^{-\frac{2}{\alpha}} 1_{\{(\frac{\pi \rho_p}{c})^{\alpha/2} < x\}} \right) + \lim_{n \rightarrow \infty} \frac{1}{n} \sum_{i=1}^n \Pr(P_i = 0).$$

(28) follows from substituting $\rho = (\lim_{n \rightarrow \infty} \frac{1}{n} \sum_{i=1}^n \Pr(P_i = 1)) \rho_p$ and the fact that $\Pr(P_i = 1) + \Pr(P_i = 0) = 1$, into the previous expression.

C. Proof of Lemma 3

Recalling that \mathcal{T} is the set of active transmitters, write (29) as

$$\begin{aligned} \frac{1}{N} \mathbf{S} \mathbf{\Psi} \mathbf{S}^\dagger &= \frac{1}{N} \sum_{i=1}^n N^{\alpha/2} R^{-\alpha} P_i \mathbf{g}_i \mathbf{g}_i^\dagger + \frac{1}{N} \sum_{i=1}^n N^{\alpha/2} (r_i^{-\alpha} - R^{-\alpha}) P_i \mathbf{g}_i \mathbf{g}_i^\dagger \\ &= \frac{N^{\frac{\alpha}{2}-1}}{R^\alpha} \sum_{i \in \mathcal{T}} \mathbf{g}_i \mathbf{g}_i^\dagger + N^{\frac{\alpha}{2}-1} \sum_{i \in \mathcal{T}} (r_i^{-\alpha} - R^{-\alpha}) \mathbf{g}_i \mathbf{g}_i^\dagger. \end{aligned} \quad (40)$$

Let $\lim_{n \rightarrow \infty} \frac{|\mathcal{T}|}{n} \rightarrow \nu$, which holds in probability from the asymptotic independence property described in Section II. ν represents the fraction of potential interferers that are active in the limit. Let the members of \mathcal{T} be labeled i_1, i_2, \dots . Next, define a new set of indices \mathcal{T}' which contains the indices of at most $\frac{3}{4}\nu n$ of the active nodes (note that any positive fraction less than one, would work here). In other words,

$$\mathcal{T}' = \left\{ i_k : k \leq \min \left(\frac{3}{4}\nu n, |\mathcal{T}| \right) \right\} \quad (41)$$

Since $c = n/N$ and $n = \pi \rho_p R^2$, $R = \sqrt{\frac{cN}{\pi \rho_p}}$. Thus, (40) can be written as

$$\frac{1}{N} \mathbf{S} \mathbf{\Psi} \mathbf{S}^\dagger = \left(\frac{\pi \rho_p}{c} \right)^{\frac{\alpha}{2}} \frac{c|\mathcal{T}'|}{n} \frac{1}{|\mathcal{T}'|} \sum_{i \in \mathcal{T}'} \mathbf{g}_i \mathbf{g}_i^\dagger + \frac{N^{\frac{\alpha}{2}-1}}{R^\alpha} \sum_{i \in \mathcal{T} \setminus \mathcal{T}'} \mathbf{g}_i \mathbf{g}_i^\dagger + N^{\frac{\alpha}{2}-1} \sum_{i \in \mathcal{T}} (r_i^{-\alpha} - R^{-\alpha}) \mathbf{g}_i \mathbf{g}_i^\dagger$$

For notational simplicity, define the following matrices

$$\mathbf{T}_1 = \left(\frac{\pi \rho_p}{c} \right)^{\frac{\alpha}{2}} \frac{c|\mathcal{T}'|}{n} \frac{1}{|\mathcal{T}'|} \sum_{i \in \mathcal{T}'} \mathbf{g}_i \mathbf{g}_i^\dagger \quad (42)$$

$$\mathbf{T}_2 = \frac{N^{\frac{\alpha}{2}-1}}{R^\alpha} \sum_{i \in \mathcal{T} \setminus \mathcal{T}'} \mathbf{g}_i \mathbf{g}_i^\dagger + N^{\frac{\alpha}{2}-1} \sum_{i \in \mathcal{T}} (r_i^{-\alpha} - R^{-\alpha}) \mathbf{g}_i \mathbf{g}_i^\dagger. \quad (43)$$

Since \mathbf{T}_2 is non-negative definite, $\lambda_{\min}(\mathbf{T}_2) \geq 0$. Thus, by the Weyl inequality (see e.g. [23]),

$$\lambda_{\min} \left(\frac{1}{N} \mathbf{S} \mathbf{\Psi} \mathbf{S}^\dagger \right) \geq \lambda_{\min}(\mathbf{T}_1) + \lambda_{\min}(\mathbf{T}_2) \geq \lambda_{\min}(\mathbf{T}_1). \quad (44)$$

Conditioned on \mathcal{D} , $\frac{|\mathcal{T}'|}{n} = \frac{3\nu}{4}$, and from Theorem 5.11 of [22], with probability 1,

$$\lambda_{\min} \left(\frac{1}{|\mathcal{T}'|} \sum_{i \in \mathcal{T}'} \mathbf{g}_i \mathbf{g}_i^\dagger \right) \rightarrow \left(1 - \sqrt{\frac{4}{3c\nu}} \right)^2 \quad (45)$$

Substituting into (42),

$$\Pr \left(\lim_{n \rightarrow \infty} \lambda_{\min}(\mathbf{T}_1) = \left(\frac{\pi \rho_p}{c} \right)^{\frac{\alpha}{2}} \frac{3c\nu}{4} \left(1 - \sqrt{\frac{4}{3c\nu}} \right)^2 \middle| \mathcal{D} \right) = 1 \quad (46)$$

The proof is completed by combining (46), (44) and Theorem 6.3 of [22], which yields that conditioned on \mathcal{D} , there exists an n_0 for which for all $n > n_0$, with probability 1,

$$\lambda_{\min} \left(\frac{1}{N} \mathbf{S} \mathbf{\Psi} \mathbf{S}^\dagger \right) \geq \lambda_{\min}(\mathbf{T}_1) \geq \left(\frac{\pi \rho_p}{c} \right)^{\frac{\alpha}{2}} \frac{3c\nu}{4} \left(1 - \sqrt{\frac{4}{3c\nu}} \right)^2. \quad (47)$$

D. Proof that HC-I and HC-II models satisfy the asymptotic independence property

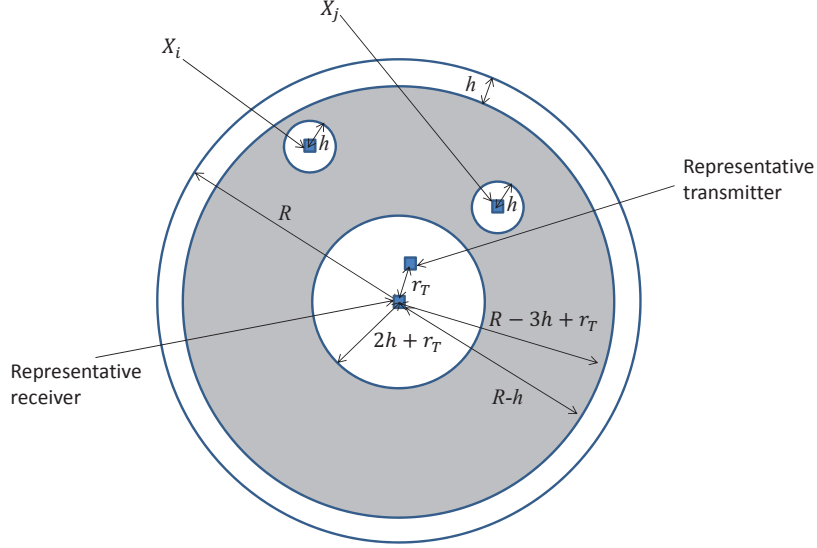


Fig. 8. Hard-core network illustrating the representative receiver, representative transmitter and two interferers.

In this section, we show that both the HC-I and HC-II models satisfy (5). Instead of showing that the joint CDFs factor in the limit, it will be simpler to show that the joint Complementary CDFs (i.e. 1-CDF) factor instead. Figure 8 illustrates the network with the representative receiver at the origin, the representative transmitter at a distance r_T from the origin, and interferers i and j . Let A denote the shaded region which is an annulus centered at the origin with inner radius $r_T + 2h$, and outer radius $R - h$. Let \mathcal{A} represent the event that $X_i \in A$, $X_j \in A$ and $|X_i - X_j| > 2h$. We consider $X_i, X_j \in A$ in order to eliminate edge effects and the effects of the representative transmitter. Note that as $R \rightarrow \infty$, $\Pr(\mathcal{A}) \rightarrow 1$ since $\Pr(X_i \in A, X_j \in A) \rightarrow 1$ as the fraction of the area of the circle of radius R that is not in A goes to zero, and the probability that the distance between two random points in A is less than $2h$ becomes negligible since this latter probability is of order $\Theta(\frac{1}{R^2})$ (e.g. see [24] Equation 2.3.63).

Since $\Pr(P_i N^{\alpha/2} r_i^{-\alpha} > x, P_j N^{\alpha/2} r_j^{-\alpha} > x) > 0$ only if $P_i = P_j = 1$, we have the following

$$\begin{aligned} & \Pr(P_i N^{\frac{\alpha}{2}} r_i^{-\alpha} > x, P_j N^{\frac{\alpha}{2}} r_j^{-\alpha} > x) \\ &= \Pr(N^{\frac{\alpha}{2}} r_i^{-\alpha} > x, N^{\frac{\alpha}{2}} r_j^{-\alpha} > x | \mathcal{A}, P_i = 1, P_j = 1) \Pr(P_i = 1, P_j = 1 | \mathcal{A}) \Pr(\mathcal{A}) \\ &+ \Pr(N^{\frac{\alpha}{2}} r_i^{-\alpha} > x, N^{\frac{\alpha}{2}} r_j^{-\alpha} > x | \mathcal{A}^c, P_i = 1, P_j = 1) \Pr(P_i = 1, P_j = 1 | \mathcal{A}^c) \Pr(\mathcal{A}^c). \end{aligned} \quad (48)$$

Since as $R \rightarrow \infty$, $\Pr(\mathcal{A}^c) \rightarrow 0$, we only need to consider the first term on the RHS of (48). The limit of this term can be found using the following two lemmas.

Lemma 4: For both the HC-I and HC-II models, and $i \neq j$, we have

$$\begin{aligned} & \lim_{n \rightarrow \infty} \Pr(N^{\frac{\alpha}{2}} r_i^{-\alpha} > x, N^{\frac{\alpha}{2}} r_j^{-\alpha} > x | \mathcal{A}, P_i = 1, P_j = 1) \\ &= \lim_{n \rightarrow \infty} \Pr(N^{\frac{\alpha}{2}} r_j^{-\alpha} > x) \lim_{n \rightarrow \infty} \Pr(N^{\frac{\alpha}{2}} r_i^{-\alpha} > x) \quad \text{and,} \end{aligned} \quad (49)$$

$$\lim_{n \rightarrow \infty} \Pr(N^{\frac{\alpha}{2}} r_i^{-\alpha} > x, | \mathcal{A}, P_i = 1) = \lim_{n \rightarrow \infty} \Pr(N^{\frac{\alpha}{2}} r_j^{-\alpha} > x) \quad (50)$$

Proof: Given in Appendix E

Lemma 5: For both the HC-I and HC-II models, and $i \neq j$,

$$\lim_{n \rightarrow \infty} \Pr(P_i = 1, P_j = 1 | \mathcal{A}) = \lim_{n \rightarrow \infty} \Pr(P_i = 1) \lim_{n \rightarrow \infty} \Pr(P_j = 1) \quad (51)$$

where $\lim_{n \rightarrow \infty} \Pr(P_i = 1) = e^{-\pi \rho_p h^2}$ and $\lim_{n \rightarrow \infty} \Pr(P_i = 1) = \frac{1 - e^{-\pi \rho_p h^2}}{\pi \rho_p h^2}$ for the HC-I and HC-II models respectively.

Proof: Given in Appendix F

Substituting $\Pr(\mathcal{A}) \rightarrow 1$, (51) and (49) into (48), and taking the limit, we have for $i \neq j$,

$$\begin{aligned} & \lim_{n \rightarrow \infty} \Pr(P_i N^{\frac{\alpha}{2}} r_i^{-\alpha} > x, P_j N^{\frac{\alpha}{2}} r_j^{-\alpha} > x) \\ &= \lim_{n \rightarrow \infty} \Pr(P_i = 1) \lim_{n \rightarrow \infty} \Pr(P_j = 1) \lim_{n \rightarrow \infty} \Pr(N^{\frac{\alpha}{2}} r_j^{-\alpha} > x) \lim_{n \rightarrow \infty} \Pr(N^{\frac{\alpha}{2}} r_i^{-\alpha} > x) \\ &= \lim_{n \rightarrow \infty} \Pr(P_j N^{\frac{\alpha}{2}} r_j^{-\alpha} > x) \lim_{n \rightarrow \infty} \Pr(P_i N^{\frac{\alpha}{2}} r_i^{-\alpha} > x), \end{aligned} \quad (52)$$

where (52) is from (49) and the fact that $\Pr(P_i = 1 | \mathcal{A}) \rightarrow \Pr(P_i = 1)$. Recalling that $p_{in} = P_i N^{\frac{\alpha}{2}} r_i^{-\alpha}$ and $p_{jn} = P_j N^{\frac{\alpha}{2}} r_j^{-\alpha}$, (52) implies (5). Additionally, $\Pr(\mathcal{A}) \rightarrow 1$ and (50) imply (10).

E. Proof of Lemma 4

Recall that \mathcal{A} is the event that $|X_i - X_j| > 2h$ and $X_i, X_j \in A$ and let $|A| = \pi(R - h)^2 - \pi(r_T + 2h)^2$ be the area of the region A . Thus,

$$\begin{aligned} & \Pr(N^{\frac{\alpha}{2}} r_i^{-\alpha} > x, N^{\frac{\alpha}{2}} r_j^{-\alpha} > x | \mathcal{A}, P_i = 1, P_j = 1) \\ &= \Pr(N^{\frac{\alpha}{2}} r_i^{-\alpha} > x | \mathcal{A}, N^{\frac{\alpha}{2}} r_j^{-\alpha} > x) \Pr(N^{\frac{\alpha}{2}} r_j^{-\alpha} > x | \mathcal{A}) \end{aligned} \quad (53)$$

Noting that \mathcal{A} implies that X_i must be outside $B(X_j, 2h)$,

$$\begin{aligned} & \Pr(N^{\frac{\alpha}{2}} r_i^{-\alpha} > x | \mathcal{A}, N^{\frac{\alpha}{2}} r_j^{-\alpha} > x) = \Pr(r_i < \sqrt{N} x^{-\frac{1}{\alpha}} | \mathcal{A}, r_j < \sqrt{N} x^{-\frac{1}{\alpha}}) \\ & \leq \left(\frac{\pi N x^{-\frac{2}{\alpha}}}{|A| - 4\pi h^2} \right) 1_{\{N^{\frac{\alpha}{2}}(R-h)^{-\alpha} \leq x \leq N^{\frac{\alpha}{2}}(r_T+2h)^{-\alpha}\}} + 1_{\{x < N^{\frac{\alpha}{2}}(R-h)^{-\alpha}\}} \\ & = \left(\frac{\pi \left(\frac{\pi \rho_p}{c} R^2\right) x^{-\frac{2}{\alpha}}}{\pi(R-h)^2 - \pi(r_T+2h)^2 - 4\pi h^2} \right) 1_{\{N^{\frac{\alpha}{2}}(R-h)^{-\alpha} \leq x \leq N^{\frac{\alpha}{2}}(r_T+2h)^{-\alpha}\}} + 1_{\{x < N^{\frac{\alpha}{2}}(R-h)^{-\alpha}\}}, \end{aligned} \quad (54)$$

where we have used $n/N = c$ and (1). Taking the limit as $n, N, R \rightarrow \infty$ and applying (1) again,

$$\lim_{n \rightarrow \infty} \Pr(N^{\frac{\alpha}{2}} r_i^{-\alpha} > x | \mathcal{A}, N^{\frac{\alpha}{2}} r_j^{-\alpha} > x) \leq \left(\frac{\pi \rho}{c} \right) x^{-\frac{2}{\alpha}} 1_{\{(\frac{\pi \rho_p}{c})^{a/2} \leq x\}} + 1_{\{x < (\frac{\pi \rho_p}{c})^{a/2}\}}.$$

Similarly, we can write a lower bound which is active if $B(X_j, 2h) \subset B(0, \sqrt{N} x^{-\frac{1}{\alpha}})$ as follows

$$\begin{aligned} & \Pr(N^{\frac{\alpha}{2}} r_i^{-\alpha} > x | \mathcal{A}, N^{\frac{\alpha}{2}} r_j^{-\alpha} > x) = \Pr(r_i < \sqrt{N} x^{-\frac{1}{\alpha}} | \mathcal{A}, r_j < \sqrt{N} x^{-\frac{1}{\alpha}}) \\ & \geq \left(\frac{\pi N x^{-\frac{2}{\alpha}} - \pi(r_T + 2h)^2 - 4\pi h^2}{|A| - 4\pi h^2} \right) 1_{\{N^{\frac{\alpha}{2}}(R-h)^{-\alpha} \leq x \leq N^{\frac{\alpha}{2}}(r_T+2h)^{-\alpha}\}} + 1_{\{x < N^{\frac{\alpha}{2}}(R-h)^{-\alpha}\}} \end{aligned}$$

Comparing with (54) and recalling that $|A| = \Theta(R^2) = \Theta(N)$, note that the lower bound converges to the same form as the upper bound as $n, N, R \rightarrow \infty$. Thus,

$$\lim_{n \rightarrow \infty} \Pr(N^{\frac{\alpha}{2}} r_i^{-\alpha} > x | \mathcal{A}, N^{\frac{\alpha}{2}} r_j^{-\alpha} > x) = \left(\frac{\pi \rho}{c} \right) x^{-\frac{2}{\alpha}} 1_{\{(\frac{\pi \rho_p}{c})^{a/2} \leq x\}} + 1_{\{x < (\frac{\pi \rho_p}{c})^{a/2}\}}. \quad (55)$$

Since X_i and X_j are independent and $\Pr(\mathcal{A}) \rightarrow 1$, from (55),

$$\lim_{n \rightarrow \infty} \Pr(N^{\frac{\alpha}{2}} r_j^{-\alpha} > x | \mathcal{A}) = \lim_{n \rightarrow \infty} \Pr(N^{\frac{\alpha}{2}} r_i^{-\alpha} > x) = \left(\frac{\pi \rho}{c} \right) x^{-\frac{2}{\alpha}} 1_{\{(\frac{\pi \rho_p}{c})^{a/2} \leq x\}} + 1_{\{x < (\frac{\pi \rho_p}{c})^{a/2}\}}.$$

Taking the limit of (53), substituting (55) and the previous expression yields (49). (50) follows directly since conditioned on \mathcal{A} , P_i is independent of the specific location of X_i , and hence r_i .

F. Proof of Lemma 5

Let $\#B(X_i, h) = |\{\ell : \ell \neq i, X_\ell \in B(X_i, h)\}|$ denote the number of potential interferers in $B(X_i, h)$ excluding the interferer at X_i itself. For both the HC-I and HC-II models, conditioned on $\#B(X_i, h) = k$ and $\#B(X_j, h) = m$, the events $P_i = 1$ and $P_j = 1$ are independent. Thus,

$$\Pr(P_i = 1, P_j = 1, \#B(X_i, h) = k, \#B(X_j, h) = m | \mathcal{A}) = \Pr(\#B(X_i, h) = k, \#B(X_j, h) = m | \mathcal{A}) \times \Pr(P_i = 1 | \mathcal{A}, \#B(X_i, h) = k) \Pr(P_j = 1 | \mathcal{A}, \#B(X_j, h) = m). \quad (56)$$

Summing (56) over all m and k excluding the potential interferers at X_i and X_j yields,

$$\Pr(P_i = 1, P_j = 1 | \mathcal{A}) = \sum_{k=0}^{n-2} \sum_{m=0}^{n-2} \Pr(P_i = 1 | \mathcal{A}, \#B(X_i, h) = k) \Pr(P_j = 1 | \mathcal{A}, \#B(X_j, h) = m) \Pr(\#B(X_i, h) = k, \#B(X_j, h) = m | \mathcal{A}). \quad (57)$$

For the HC-I model, $P_i = 1$ and $P_j = 1$ if and only if $\#B(X_i, h) = 0$ and $\#B(X_j, h) = 0$, respectively. Hence (57) becomes

$$\begin{aligned} \Pr(P_i = 1, P_j = 1 | \mathcal{A}) &= \Pr(\#B(X_i, h) = 0, \#B(X_j, h) = 0 | \mathcal{A}) \\ &= \Pr(\#B(X_i, h) = 0 | \mathcal{A}, \#B(X_j, h) = 0) \Pr(\#B(X_j, h) = 0, \mathcal{A}). \end{aligned} \quad (58)$$

Recall that conditioned on \mathcal{A} , $X_i \notin B(X_j, h)$, and $P_j = 1$ if the $n - 2$ remaining potential interferers are not in $B(X_j, h)$. Using the fact that $n = \pi \rho_p R^2$ we have

$$\lim_{n \rightarrow \infty} \Pr(\#B(X_j, h) = 0 | \mathcal{A}) = \lim_{R \rightarrow \infty} \left(1 - \frac{\pi h^2}{\pi R^2}\right)^{\pi \rho_p R^2 - 2} = e^{-\pi \rho_p h^2}. \quad (59)$$

Furthermore, since $\Pr(\mathcal{A}) \rightarrow 1$ as $n, N, R \rightarrow \infty$, we have

$$\lim_{n \rightarrow \infty} \Pr(P_j = 1) = \lim_{n \rightarrow \infty} [\Pr(\#B(X_j, h) = 0 | \mathcal{A}) \Pr(\mathcal{A}) + \Pr(P_j = 1, \mathcal{A}^c)] = e^{-\pi \rho_p h^2}. \quad (60)$$

Conditioned on $\#B(X_j, h) = 0$ the $n - 2$ potential interferers are outside $B(X_j, h)$. Since $P_i = 1$ only if the remaining $n - 2$ potential interferers are outside $B(X_i, h)$ as well,

$$\begin{aligned} \Pr(\#B(X_i, h) = 0 | \mathcal{A}, \#B(X_j, h) = 0) &= \left(1 - \frac{\pi h^2}{\pi R^2 - \pi h^2}\right)^{\pi \rho_p R^2 - 2}, \\ \lim_{n \rightarrow \infty} \Pr(\#B(X_i, h) = 0 | \mathcal{A}, \#B(X_j, h) = 0) &= e^{-\pi \rho_p h^2} = \lim_{n \rightarrow \infty} \Pr(P_i = 1) \end{aligned} \quad (61)$$

where the last equality follows from symmetry between X_i and X_j and (60). Substituting (60) and (61) into (58) and taking the limit yields (51) for the HC-I model.

For the HC-II model, using the fact that $\Pr(P_i = 1 | \#B(X_i, h) = k, \mathcal{A}) = \frac{1}{k+1}$, (57) becomes

$$\begin{aligned} \Pr(P_i = 1, P_j = 1 | \mathcal{A}) &= \sum_{k=0}^{n-2} \sum_{m=0}^{n-2} \frac{1}{(k+1)(m+1)} \Pr(\#B(X_i, h) = k, \#B(X_j, h) = m | \mathcal{A}), \\ &= \sum_{k=0}^{n-2} \frac{1}{k+1} \Pr(\#B(X_i, h) = k | \mathcal{A}) \sum_{m=0}^{n-k-2} \frac{1}{m+1} \Pr(\#B(X_j, h) = m | \#B(X_i, h) = k, \mathcal{A}), \\ &= \sum_{k=0}^{n-2} \frac{1}{k+1} \binom{n-2}{k} \left(\frac{\pi h^2}{\pi R^2}\right)^k \left(1 - \frac{\pi h^2}{\pi R^2}\right)^{n-k-2} \times \\ &\quad \sum_{m=0}^{n-k-2} \frac{1}{m+1} \binom{n-k-2}{m} \left(\frac{\pi h^2}{\pi R^2 - \pi h^2}\right)^m \left(1 - \frac{\pi h^2}{\pi R^2 - \pi h^2}\right)^{n-k-2-m} \end{aligned} \quad (62)$$

Consider the previous expression written in terms of a double series (please see e.g. [25] for basic properties of double series) with the variables n_1 and n_2 replacing n , in the terms in the summation, and the upper limit of the summation respectively. Additionally, since $R = \sqrt{\frac{n}{\pi\rho_p}}$,

$$\Pr(P_i = 1, P_j = 1|\mathcal{A}) = \sum_{k=0}^{n_2-2} \frac{1}{k+1} \binom{n_1-2}{k} \left(\frac{h^2}{n_1/\rho_p}\right)^k \left(1 - \frac{h^2}{n_1/\rho_p}\right)^{n_1-k-2} \times \sum_{m=0}^{n_2-k-2} \frac{1}{m+1} \binom{n_1-k-2}{m} \left(\frac{h^2}{n_1/\rho_p - h^2}\right)^m \left(1 - \frac{h^2}{n_1/\rho_p - h^2}\right)^{n_1-k-2-m} \quad (63)$$

Taking the limits of (63) as $n_1 \rightarrow \infty$ followed by $n_2 \rightarrow \infty$, we have

$$\lim_{n_2 \rightarrow \infty} \lim_{n_1 \rightarrow \infty} \Pr(P_i = 1, P_j = 1|\mathcal{A}) = \lim_{n_2 \rightarrow \infty} \sum_{k=0}^{n_2-2} \frac{(\pi\rho_b h^2)^k e^{-\pi h^2 \rho_p}}{(k+1)!} \sum_{m=0}^{n_2-k-2} \frac{(\pi\rho_b h^2)^m e^{-\pi h^2 \rho_p}}{(m+1)!} \quad (64)$$

$$\lim_{n_2 \rightarrow \infty} \lim_{n_1 \rightarrow \infty} \Pr(P_i = 1, P_j = 1|\mathcal{A}) = \left(\frac{1 - e^{-\pi h^2 \rho_p}}{\pi\rho_b h^2}\right)^2 \quad (65)$$

Since both the sums on the RHS of (64) are finite for all n_2 , by Theorem 2.11 of [25],

$$\begin{aligned} \lim_{n \rightarrow \infty} \Pr(P_i = 1, P_j = 1|\mathcal{A}) &= \lim_{n_1, n_2 \rightarrow \infty} \Pr(P_i = 1, P_j = 1|\mathcal{A}) \\ &= \lim_{n_2 \rightarrow \infty} \lim_{n_1 \rightarrow \infty} \Pr(P_i = 1, P_j = 1|\mathcal{A}) = \left(\frac{1 - e^{-\pi h^2 \rho_p}}{\pi\rho_b h^2}\right)^2. \end{aligned} \quad (66)$$

Following similar steps, we have

$$\lim_{n \rightarrow \infty} \Pr(P_i = 1) = \lim_{n \rightarrow \infty} \Pr(P_j = 1) = \frac{1 - e^{-\pi h^2 \rho_p}}{\pi\rho_b h^2}. \quad (67)$$

Substituting (67) into (65) yields (51) completing the proof.

G. Proof that Frequency Reuse Model Satisfies Asymptotic Independence Criteria

Let \mathcal{B} denote the event that X_i and X_j are in cells assigned to band 0 which are wholly contained in $B(0, R)$, and X_i and X_j are in different cells. The event \mathcal{B} can be described as: $\exists k, \ell$ such that $X_i \in \mathcal{C}_k, X_j \in \mathcal{C}_\ell, \mathcal{C}_k \subset B(0, R), \mathcal{C}_\ell \subset B(0, R)$ and $k \neq \ell$. Note that $\Pr(\mathcal{B}) \rightarrow \frac{1}{\kappa^2}$ as $R \rightarrow \infty$, since the probability that X_i or X_j are in a cell assigned to band zero approaches $\frac{1}{\kappa}$, and the probability that they are in the same cell goes to zero. Let \mathcal{C}_A denote the union of all cells wholly contained in $B(0, R)$, i.e. $\mathcal{C}_A = \bigcup_{k: \mathcal{C}_k \subset B(0, R)} \mathcal{C}_k$. Now consider the following

$$\begin{aligned} \frac{|\mathcal{C}_A \cap B(0, \sqrt{N}x^{-\frac{1}{\alpha}})| - |\mathcal{C}_0|}{|\mathcal{C}_A| - |\mathcal{C}_0|} &\leq \Pr\left(P_i^{-\frac{1}{\alpha}} r_i < \sqrt{N}x^{-\frac{1}{\alpha}} | P_j^{-\frac{1}{\alpha}} r_j < \sqrt{N}x^{-\frac{1}{\alpha}}, \mathcal{B}, P_i = 1, P_j = 1\right) \\ &\leq \frac{|\mathcal{C}_A \cap B(0, \sqrt{N}x^{-\frac{1}{\alpha}})|}{|\mathcal{C}_A| - |\mathcal{C}_0|} \end{aligned} \quad (68)$$

The lower bound holds when the cell containing X_j is a subset of $B(0, \sqrt{N}x^{-\frac{1}{\alpha}})$. The upper bound holds if the cell containing X_j intersects with $B(0, \sqrt{N}x^{-\frac{1}{\alpha}})$ at a single point X_j . As $R \rightarrow \infty$, the edge effects diminish, and the upper and lower bounds converge to same form:

$$\lim_{n \rightarrow \infty} \frac{|\mathcal{C}_A \cap B(0, \sqrt{N}x^{-\frac{1}{\alpha}})|}{|\mathcal{C}_A|} = \left(\frac{\pi\rho}{c} x^{-\frac{2}{\alpha}}\right) 1_{\left\{(\frac{\pi\rho_p}{c})^{a/2} \leq x\right\}} = \Pr(r_i < \sqrt{N}x^{-\frac{1}{\alpha}}) \quad (69)$$

which implies that

$$\lim_{n \rightarrow \infty} \Pr \left(P_i^{-\frac{1}{\alpha}} r_i < \sqrt{N} x^{-\frac{1}{\alpha}} | \mathcal{B}, P_j^{-\frac{1}{\alpha}} r_j < \sqrt{N} x^{-\frac{1}{\alpha}}, P_i = 1, P_j = 1 \right) = \Pr \left(r_i < \sqrt{N} x^{-\frac{1}{\alpha}} \right). \quad (70)$$

Following similar steps, we can show the following

$$\lim_{n \rightarrow \infty} \Pr \left(P_j^{-\frac{1}{\alpha}} r_j < \sqrt{N} x^{-\frac{1}{\alpha}} | \mathcal{B}, P_i = 1, P_j = 1 \right) = \Pr(r_j < \sqrt{N} x^{-\frac{1}{\alpha}}) \quad (71)$$

$$\lim_{n \rightarrow \infty} \Pr \left(P_i^{-\frac{1}{\alpha}} r_i < \sqrt{N} x^{-\frac{1}{\alpha}} | X_i \in \mathcal{C}_A, P_i = 1 \right) = \Pr(r_i < \sqrt{N} x^{-\frac{1}{\alpha}}) \quad (72)$$

Since as $n, N, R \rightarrow \infty$, $\Pr(\mathcal{A} | P_i = 1) \rightarrow 1$, (72) implies (10). Recalling that if \mathcal{B} holds, X_i and X_j are in different cells and the probability that $P_i = 1$ if there are k additional potential interferers in the cell containing X_i is $\frac{1}{k+1}$, we have the following

$$\begin{aligned} & \Pr(P_i = 1, P_j = 1 | \mathcal{B}, m \text{ additional potential interferers in cell containing } X_j) \\ &= \frac{1}{m+1} \sum_{k=0}^{n-m-2} \frac{1}{k+1} \binom{n-m-2}{k} \left(\frac{|\mathcal{C}_0|}{\pi R^2 - |\mathcal{C}_0|} \right)^k \left(1 - \frac{|\mathcal{C}_0|}{\pi R^2 - |\mathcal{C}_0|} \right)^{n-m-k-2} \end{aligned}$$

Multiplying by $\Pr(\text{mpotential interferers in the cell containing } X_j | \mathcal{B})$, and summing over m ,

$$\begin{aligned} \Pr(P_i = 1, P_j = 1 | \mathcal{B}) &= \sum_{m=0}^{n-2} \frac{1}{m+1} \binom{n-2}{m} \left(\frac{|\mathcal{C}_0|}{\pi R^2} \right)^m \left(1 - \frac{|\mathcal{C}_0|}{\pi R^2} \right)^{n-2-m} \\ &\times \sum_{k=0}^{n-2-m} \frac{1}{k+1} \binom{n-m-2}{k} \left(\frac{|\mathcal{C}_0|}{\pi R^2 - |\mathcal{C}_0|} \right)^k \left(1 - \frac{|\mathcal{C}_0|}{\pi R^2 - |\mathcal{C}_0|} \right)^{n-m-2-k} \end{aligned} \quad (73)$$

Note the similarity of (73) and (62). Following steps used to derive (66), it can be shown that

$$\lim_{n \rightarrow \infty} \Pr(P_i = 1, P_j = 1 | \mathcal{B}) = \left(\frac{1 - e^{-|\mathcal{C}_0| \rho_p}}{|\mathcal{C}_0| \rho_p} \right)^2 \quad (74)$$

$$\lim_{n \rightarrow \infty} \Pr(P_i = 1, |X_i \in \mathcal{C}_A) = \frac{1 - e^{-|\mathcal{C}_0| \rho_p}}{|\mathcal{C}_0| \rho_p} \quad (75)$$

Taking the product of (72) and (75), substituting (69), and using the fact that $\Pr(X_i \in \mathcal{C}_A) \rightarrow \frac{1}{\kappa}$,

$$\lim_{n \rightarrow \infty} \Pr \left(P_i r_i^{-\alpha} N^{\frac{\alpha}{2}} \leq x \right) = \frac{1}{\kappa} \left(\frac{1 - e^{-|\mathcal{C}_0| \rho_p}}{|\mathcal{C}_0| \rho_p} \right) \left(\frac{\pi \rho}{c} x^{-\frac{2}{\alpha}} \right) 1_{\left\{ \left(\frac{\pi \rho_p}{c} \right)^{a/2} \leq x \right\}} \quad (76)$$

As $R \rightarrow \infty$, $\Pr(P_i = 1, P_j = 1 | \mathcal{B}^c) \rightarrow 0$, because the probability that X_i and X_j are in the same cell $\rightarrow 1$, which means that in the limit, \mathcal{B}^c holds only when X_i or X_j are not in cells assigned to band 0. Taking the product of (70), (71), (74) and $\lim_{n \rightarrow \infty} \Pr(\mathcal{B}) = \frac{1}{\kappa^2}$ yields,

$$\lim_{n \rightarrow \infty} \Pr \left(P_i r_i^{-\alpha} N^{\frac{\alpha}{2}} > x, P_j r_j^{-\alpha} N^{\frac{\alpha}{2}} > x \right) = \frac{1}{\kappa^2} \left(\frac{\pi \rho}{c} x^{-\frac{2}{\alpha}} \right)^2 \left(\frac{1 - e^{-|\mathcal{C}_0| \rho_p}}{|\mathcal{C}_0| \rho_p} \right)^2 \quad (77)$$

$$= \lim_{n \rightarrow \infty} \Pr \left(P_i r_i^{-\alpha} N^{\frac{\alpha}{2}} > x \right) \lim_{n \rightarrow \infty} \Pr \left(P_j r_j^{-\alpha} N^{\frac{\alpha}{2}} > x \right). \quad (78)$$

Recalling the definitions of p_{in} and p_{jn} , (78) implies (5). Substituting the density of cells $\rho_c = \frac{1}{|\mathcal{C}_0|}$, into (75) and observing that $\Pr(X_i \in \mathcal{C}_A) \rightarrow \frac{1}{\kappa}$ yields the effective density ρ in (20).

REFERENCES

- [1] S. Govindasamy, D. Bliss, and D. Staelin, "Spectral efficiency in single-hop ad-hoc wireless networks with interference using adaptive antenna arrays," *IEEE J. Sel. Areas Commun.*, vol. 25, no. 7, pp. 1358–1369, Sep. 2007.
- [2] N. Jindal, J. Andrews, and S. Weber, "Multi-antenna communication in ad hoc networks: Achieving MIMO gains with SIMO transmission," *IEEE Trans. Commun.*, vol. 59, no. 2, pp. 529–540, Feb. 2011.
- [3] O. Ali, C. Cardinal, and F. Gagnon, "Performance of optimum combining in a Poisson field of interferers and Rayleigh fading channels," *IEEE Trans. Wireless Commun.*, vol. 9, no. 8, pp. 2461–2467, Aug. 2010.
- [4] R. Louie, M. McKay, and I. Collings, "Open-loop spatial multiplexing and diversity communications in ad hoc networks," *IEEE Trans. Inf. Theory*, vol. 57, no. 1, pp. 317–344, Jan. 2011.
- [5] Y. Wu, R. H. Y. Louie, M. R. McKay, and I. B. Collings, *IEEE Trans. Wireless Commun.*, vol. 11, no. 8, pp. 2815–2827, Aug. 2012.
- [6] J. G. Andrews, F. Baccelli, and R. K. Ganti, "A tractable approach to coverage and rate in cellular networks," *IEEE Trans. Commun.*, vol. 59, no. 11, pp. 3122–3134, Apr. 2011.
- [7] M. Haenggi, "Mean interference in hard-core wireless networks," *IEEE Commun. Lett.*, vol. 15, no. 8, Aug. 2011.
- [8] R. Ganti, J. Andrews, and M. Haenggi, "High-SIR transmission capacity of wireless networks with general fading and node distribution," *IEEE Trans. Inf. Theory*, vol. 57, no. 5, May 2011.
- [9] R. Giacomelli, R. Ganti, and M. Haenggi, "Outage probability of general ad hoc networks in the high-reliability regime," *IEEE/ACM Trans. Netw.*, vol. 19, no. 4, pp. 1151–1163, Aug. 2011.
- [10] A. Hunter, R. Ganti, and J. Andrews, "Transmission capacity of multi-antenna ad hoc networks with CSMA," in *Conference Record of the 44th Asilomar Conference on Signals, Systems and Computers*, Nov. 2010.
- [11] T. D. Novlan, H. S. Dhillon, and J. G. Andrews, "Analytical modeling of uplink cellular networks," *CoRR*, vol. abs/1203.1304, 2012.
- [12] W. Xiao, R. Ratasuk, A. Ghosh, R. Love, Y. Sun, and R. Nory, "Uplink power control, interference coordination and resource allocation for 3GPP E-UTRA," in *Proc. IEEE Vehicular Technology Conference*, Sep. 2006, pp. 1–5.
- [13] S. Govindasamy, D. W. Bliss, and D. H. Staelin, "Asymptotic spectral efficiency of the uplink in spatially distributed wireless networks with multi-antenna base stations," to appear, *IEEE Trans. Commun.*, 2013. [Online]. Available: <http://arxiv.org/abs/1102.1232>
- [14] R. Ganti and M. Haenggi, "Interference and outage in clustered wireless ad hoc networks," *IEEE Trans. Inf. Theory*, vol. 55, no. 9, pp. 4067–4086, Sep. 2009.
- [15] R. Tresch and M. Guillaud, "Clustered interference alignment in large cellular networks," in *IEEE International Symposium on Personal, Indoor and Mobile Radio Communications (PIMRC)*, 2009.
- [16] M. Abramovitz and I. Stegun, *Handbook of Mathematical Functions*. Dover Publications, New York, 1970.
- [17] S. Govindasamy, D. W. Bliss, and D. H. Staelin, "Asymptotic spectral efficiency of multi-antenna links in wireless networks with limited Tx CSI," *IEEE Trans. Inf. Theory*, Aug. 2012.
- [18] D. Stoyan, W. S. Kendall, and J. Mecke, *Stochastic Geometry and Its Applications*. John Wiley and Sons, 1995.
- [19] F. Baccelli and B. Błaszczyszyn, *Stochastic Geometry and Wireless Networks, Volume I - Theory*, ser. Foundations and Trends in Networking Vol. 3: No 3-4, pp 249-449. NoW Publishers, 2009, vol. 1.
- [20] T. D. Novlan, H. S. Dhillon, and J. G. Andrews, "Analytical modeling of uplink cellular networks," *CoRR*, vol. abs/1203.1304, 2012.
- [21] S. Hanly and D. Tse, "Resource pooling and effective bandwidths in CDMA systems with multiuser receivers and spatial diversity," *IEEE Trans. Inform. Theory*, vol. 47, no. 4, pp. 1328–1351, May 2001.
- [22] Z. Bai and J. Silverstein, *Spectral analysis of large dimensional random matrices*. Springer, 2009.
- [23] R. Horn and C. R. Johnson, *Matrix Analysis*. Cambridge University Press, 1990.
- [24] A. M. Mathai, *An Introduction to Geometrical Probability*. Gordon and Breach Science Publishers, 1999.
- [25] E. D. Habil, "Double sequences and double series," *Islamic University Journal-Series of Natural Studies and Engineering*, vol. 14, no. 1, pp. 223–254, 2006.